DOI: 10.4408/IJEGE.2011-03.B-037

PORE WATER PRESSURE DISTRIBUTIONS OF GRANULAR MIXTURE FLOW IN A ROTATING MILL

Norifumi HOTTA(*)

(*)Graduate School of Life and Environmental Sciences, University of Tsukuba (1-1-1 Tennodai, Tsukuba, Ibaraki 3058577, Japan)

ABSTRACT

We measured the pore water pressure distributions in miniature debris flows to assess the validity of the related constitutive equations. Our experiments used a rotating mill that allowed steady flows to be maintained easily and a Pitot tube to measure pore pressure accurately. Plastic and glass beads with particle sizes of 1–6 mm were used to simulate the debris flows. Since laboratory debris flows within a rotating mill give flow fields that differ from those of in situ debris flows, the flow characteristics in the rotating mill were also investigated. The experimental results showed that the pore water pressure was greater than the hydrostatic pressure. Although Stokes drag also appeared in the excess pore pressure in tests of small particle sizes due to infiltration flow caused by the inherent fluid field of the granular mixture flows in the rotating mill, pore water pressure in the case of 6-mm particles could be induced by Reynolds stress. The observed excess pore water pressure in the debris flows with 6-mm particles corresponded closely to theoretical values, supporting the use of constitutive equations for evaluating shear stress in the pore fluid of debris flows.

Key words: *constitutive equation, debris flow, pore pressure, Reynolds stress, rotating mill*

INTRODUCTION

Debris flows exhibit various fluidities, due to the material condition of the contained sediment (e.g., size, specific weight,friction coefficient, and coefficient of restitution) and sediment concentration. Thus, many different kinds of debris flows are possible, such as boulder debris flow (Takahashi, 1977; Tsubaki *et alii*, 1982; Egashira *et alii*, 1989), hyper-concentrated flow (Arai & Takahashi, 1986; Winterwerp *et alii,* 1990), and mud flow (O'Brien & Julien, 1988; Shanmugam, 1996). These flows are usually classified based on phenomenal behavior without a clear definition of the mechanics.

The basic nature of debris flow as a multiphase flow can be described using constitutive equations (Takahashi, 1977; Tsubaki *et alii*, 1982; Egashira *et alii*, 1997), which have been derived from simple modeling of the laminar motion of sediment particles, focusing on the stress structure of the particles and the pore fluid. These equations have been experimentally validated, for example, by comparing theoretical and experimental velocity distributions (Itoh & Egashira, 1999) and flow resistance (Arattano & Franzi, 2004). However, those indices as measures of velocity distributions and flow resistance were merely comprehensive indices that resulted from the internal stress structure. Few studies have succeeded in directly measuring internal stresses, with some exceptions including Bagnold (1954) and Miyamoto (1985) who measured the pressure component due to particle-to-particle collisions in granular flows.

Rickenmann (1991) and Takahashi & Kobayashi (1993) investigated how increasing fluid viscosity

with clay suspensions affected the fluidity of debris flows containing coarse particles, in which the viscous coefficient of pore fluid altered the total shear stress. Egashira *et alii* (1989) investigated boulder debris flows in which pore fluid can be treated as clear water by formulating Reynolds stress in the pore fluid as a component of shear stresses, based on the idea that pore fluid is turbulent, resulting from strong shear induced by sediment particles, although sediment particles themselves descend in a laminar motion.

While excess pore pressure in debris flows, including fine sediment, has been examined (Savage & Iverson, 2003; Iverson *et alii*, 2010), pore water pressure in boulder debris flows has often been regarded as hydrostatic. This should not be the case when Reynolds stress is present as shear stress. Assuming an isotropic turbulent condition in the pore fluid of debris flows makes it possible to consider pore pressures to be greater than hydrostatic pressure, due to Reynolds stress being the same as the shear stress. Iverson (1997), Imaizumi *et alii* (2003), and McArdell *et alii* (2007) observed excess pore pressure from hydrostatic pressure in mature debris flows. Their results incorporated the presence of the Reynolds stress component in pressure. This is noteworthy because measuring pore water pressure makes it possible to estimate the shear stress component of Reynolds stress, which is considered to be present to the same extent as described above. Above all, measuring pore water pressure may explain the stress structure of debris flows. Egashira *et alii* (1997) proposed a constitutive equation for debris flow, which consisted of stress terms relating sediment particle-toparticle collisions, friction between sediment particles, and Reynolds stress due to pore fluid mixing. Because the sum of the three stress components equals the external force, and the stress from particle-to-particle collisions among the three stresses can be validated (Miyamoto, 1985), measuring either of the two unknown stresses experimentally can reveal total stress.

Pore water pressure measurements are difficult for debris flows under various conditions during field observations or in large scale experiments. Even if they are attempted, it is particularly difficult to assess the internal structure of debris flows, because only basal pore water pressure can be measured in such debris flows. Consequently, laboratory testing is the most suitable method for measuring detailed pore water pressure in debris flows. Even in the laboratory setting, accurate measurements of pore water pressure distributions in an open channel are difficult, because collisions of sediment particles with pressure gauges can influence measurements. To avoid this, Hotta & Ohta (2000) used a rotating mill to measure pore water pressure distributions in laboratory debris flows. Rotating mills (also known as tumbling mills) have been used frequently for laboratory abrasion experiments (Krumbein, 1941; Kuenen, 1956). The debris flow within a rotating mill can be maintained in a relatively stationary manner. Although internal particles are agitated within the rotating mill, the effect of particle collisions with sensing instruments is greatly reduced compared with that in an open channel. Additionally, a steady flow can be easily maintained in the rotating mill with only slight fluctuations in flow surface, allowing steady measurement of pore water pressure. However, Hotta *et alii* (1998) noted that the measured pore water pressure might be affected by factors other than Reynolds stress, including centrifugal force and infiltration flow, so laboratory debris flows produced in rotating mills may have a different nature from actual debris flows. In this study, we measured pore water pressure distributions in laboratory debris flows in a rotating mill to investigate the internal stresses of debris flows. First, differences in flow fields were specified between debris flows in the rotating mill and actual debris flows to obtain adequate experimental conditions for measuring pore water pressure. Based on these experimental results, we assessed the validity of constitutive equations for debris flows, which assume pore water pressure based on related stress components

PORE-WATER PRESSURE IN DEBRIS FLOWS

Pore water pressure in a debris flow pw can be expressed as follows:

$$p_w = p_h + p_f \tag{1}$$

where p_h is the hydrostatic pressure and p_f is the Reynolds stress from turbulent mixing in pore water. Turbulence in the pore space of debris flows is strongly affected by particle shearing. Based on Prandtl's mixing length theory, p_f can be rewritten as:

$$p_f = \rho\overline{u'u'} = \rho l^2\left(\frac{\partial u}{\partial z}\right)^2 \quad (2)$$

p is the density of pore water, u' is the fluctuation velocity of pore water, l is the mixing length in the pore space, and u is the mean velocity of pore water, which is assumed to correspond with debris flow velocity. Note that this is a very simple assumption as pore water in debris flows is strongly sheared by particles. In debris flows, l is defined by the scale of the pore space. Ashida *et al.* (1985) proposed the following expression for l:

$$l = \sqrt{k_f}\left(\frac{1-c}{c}\right)^{1/3} d \quad (3)$$

where k_f is the ratio between shape parameters for the sediment particle and the pore space in the range of 0.16-0.25 (Ashida *et alii*, 1985; Egashira *et alii*, 1989), c is the sediment concentration, and d is the diameter of sediment particles. Ashida *et alii* (1985) expressed kf as:

$$\sqrt{k_f} = \left(k_p/k_v\right)^{1/3},\ k_p = \frac{V_p}{d^3},\ k_v = \frac{V_v}{L^3} \quad (4)$$

where k_p and k_v are the shape coefficient of sediment particles and pore space, respectively, V_p and V_v are the volumes of sediment particles and pore space in unit volume, and L is the length scale of the pore space. Substituting eq. (3) into eq. (2) yields the following expression for p_f:

$$p_f = k_f \rho d^2 \frac{(1-c)^{2/3}}{c^{2/3}}\left(\frac{\partial u}{\partial z}\right)^2 \quad (5)$$

The vertical velocity profile appears in eq. (5). Although the constitutive equations should be solved to obtain an exact velocity profile for debris flows, an approximation for boulder debris flows can be readily generated. When steady and uniform debris flows descend with a uniform sediment particle size and uniform sediment concentration profile, shear stress τ is balanced with external force as follows:

$$\tau(z) = K(c,d)\left(\frac{\partial u}{\partial z}\right)^2 = \int_z^h \rho_m g \sin\theta\, dz = \rho_m g \sin\theta (h-z) \quad (6)$$

where $K(c, d)$ is the function of c and d, which is derived from the constitutive equations of debris flow (Hotta & Miyamoto, 2008), ρ_m is the mass density of the debris flow, g is the acceleration due to gravity, θ is the inclination, and h is the flow depth. Assuming a uniform sediment concentration, the velocity profile can be given by integrating eq. (6) as follows:

$$u = \frac{2}{3} h \sqrt{\frac{\rho_m g h \sin\theta}{K(c,d)}}\left\{1-\left(1-\frac{z}{h}\right)^{3/2}\right\} \quad (7)$$

Equation (7) exhibits the typical velocity profile for a dilatant fluid in an open channel (Takahashi, 1977) and can be rewritten using the mean velocity u_m as follows:

$$u = \frac{5}{3} u_m \left\{1-\left(1-\frac{z}{h}\right)^{3/2}\right\} \quad (8)$$

Differentiating eq. (8) and substituting into eq. (5) yields the following expression for the theoretical p_f profile:

$$p_f = k_f \rho d^2 \frac{(1-c)^{2/3}}{c^{2/3}} \frac{25 u_m^{\ 2}}{4h^2}\left(1-\frac{z}{h}\right) \quad (9)$$

According to eq. (9), pf distributes linearly from the flow surface to the bed, and p_f increases in proportion to the square of d and u_m, respectively, when the sediment concentration profile is uniform.

EXPERIMENTAL METHODS AND MATERIALS

The rotating mill was 4 cm wide and 20 cm in diameter; it was constructed of an acrylic cylinder and discs (Fig. 1). Glass beads (4 mm in diameter)

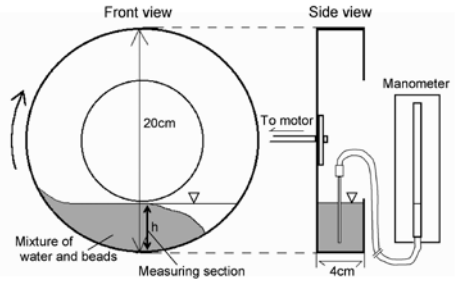

Fig. 1 - Sketch of the experimental setup

	Specific weight (g/cm^3)	Diameter (mm)
Glass beads	2.37	1, 2, 3, 4, 5, 6
Plastic beads	1.38	4, 6

Tab. 1. Materials used in the experiment.

were glued inside the cylinder to simulate bed roughness. The rotating mill was connected to a motor via a gear box, and the rotating speed was controlled by changing the power supply voltage. The Pitot tube used to measure pore water pressure was constructed of a stainless tube (1.5 mm external diameter, 1.0 mm bore diameter). The end of this tube was closed and an opening (0.8 mm in diameter) was made in both lateral faces near the end. The Pitot tube was placed into the rotating mill vertically with the opening facing perpendicular to the flow direction to measure the static pore water pressure profile. Although the rotating mill reduces the influence of particle collisions with the Pitot tube, it remains possible that the Pitot tube itself disturbs the surrounding flow, which will affect the measurements. However, no apparent disturbance was observed under the experimental conditions in this study.

Table 1 lists the materials used in the experiments. Each type of material (50 cm^3) was mixed with water (130 cm^3) to form a mixture (180 cm^3). Based on the mixing ratio, the concentration of the mixture was 0.28, but the granular mixture flow maintained in the rotating mill resulted in separation of the water phase and the mixture phase in the front part (see Fig. 1), resulting in a mean concentration greater than 0.28 for the debris-flow part.

After the mixture was poured into the mill, the pore water pressure profile was measured during a constant rotational speed. Pore water pressure was measured vertically at the center line of the rotating mill at heights of every 2 or 3 mm, with the bed surface set as the bottom (0 mm). The speed of rotation was recorded and checked before and after measurements to confirm the flow was steady.

After experiments were completed, the velocity profile and mean concentration of each granular mixture flow was examined by analyzing images recorded by a video camera. The velocity profile was obtained by chasing the trajectories of particles passing through the measuring section. The mean concentration was obtained from the ratio between the projected area of the debris flow phase (mixture phase) and the water phase, which are separated in the rotating mill, as described previously. Because the volume of the beads and water was known, comparison of the projected areas enabled estimation of the mean concentration of the granular mixture flow, assuming a uniform concentration in the debris flow part (Hotta & Ohta, 2000).

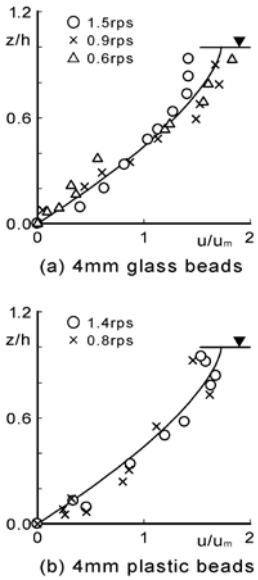

Fig.2 - Nondimensional velocity profiles measured in the rolling mill. The velocity of the glued beads of bed roughness, which was equal to the rotating speed, was set as zero. Solid curve indicates theoretical velocity profile for boulder debris flows

RESULTS

VELOCITY PROFILE

Figure 2 shows the velocity profiles of the granular mixture flows in the rotating mill. The velocity of the glued beads to simulate bed roughness, which was equal to the speed of rotation, was set at zero. Although in some cases a velocity deficit appeared near the flow surface, velocity profiles of both plastic and glass beads corresponded well with the theoretical velocity profile of a boulder debris flow, described in eq. (8).

To visualize internal flow in the water phase, metal powder was placed in the rotating mill in some experiments (see Fig. 3 for an overview). The dominant current in the water phase was induced at the meeting point of the debris flow front and the bed surface. Because these two motions were in opposite directions, the collisions generated a complex current circulating in the water phase. A current also emerged from the debris flow surface, generated by debouched pore water (Fig. 3).

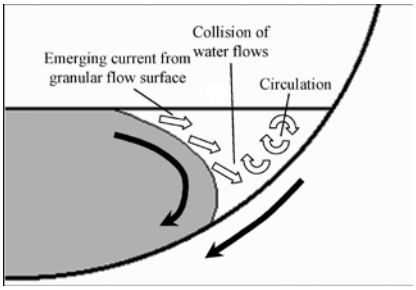

Fig. 3 - Schematic illustration of internal flows in water phase

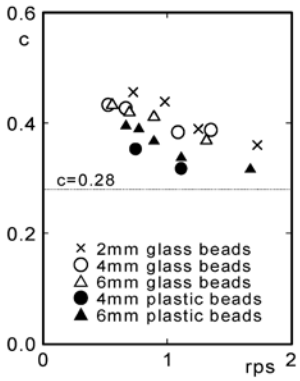

Fig. 4 - Relationship between speed of rotation (rps) and mean concentration in laboratory debris flows

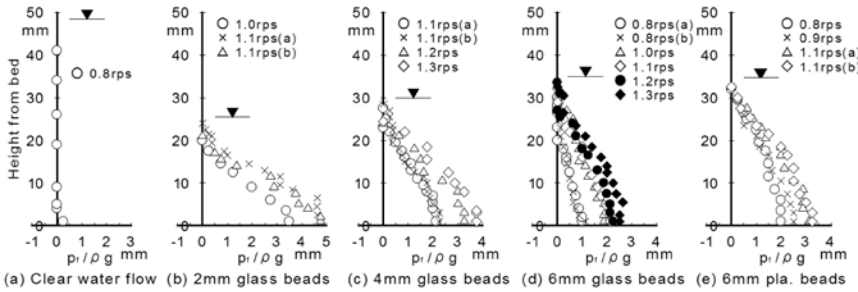

Fig. 5 - Excess pore water pressure distributions

MEAN CONCENTRATION

Mean concentrations of granular mixture flows varied due to the differing materials and the rotating mill's speed of rotation. Figure 4 shows the relationship between mean concentration and speed of rotation (rps, revolutions per second); it also indicates the minimum mean concentration (c = 0.28) derived simply from the mixing ratio of the mixture. The figure shows that granular mixture flows had a higher mean concentration of glass beads than plastic beads. For glass beads with a comparable speed of rotation, the highest concentrations were observed when 2-mm particles were used, and no significant difference was detected between glass beads of 4 mm and 6 mm. In contrast, mean concentrations in mixtures of plastic beads were higher for 6-mm particles than for 4-mm particles. Mixtures of glass and plastic beads both exhibited the same trend of lower concentrations during faster speeds of rotation

PORE-WATER PRESSURE

Figure 5 shows the vertical distribution of excess pore water pressure from hydrostatic pressure, with pf converted into water height (mm). Figure 5a also shows the p_f distribution for clear water flow as a control. While the p_f in clear water was nearly zero, resulting in hydrostatic pressure at any depth in the flow, the pf in all granular mixture flows began to increase from the flow surface to the bed, indicating greater pore water pressure than hydrostatic pressure. The distribution had a roughly linear shape in most cases, while some cases resulted in a parabolic profile with moderate increases in pf near the bed (Fig. 5d). The pore water pressure observed in real debris flows is often high enough to support the total pressure of debris flow (Imaizumi *et alii*, 2003; McArdell *et alii*, 2007; Iverson *et alii*, 2010), resulting in a fully liquefied state. However, the excess pore pressure shown in Figure 5 is too low to support the weight of the beads completely, indicating that internal stresses due to particles are dominant in these experimental conditions.

When the type of material remained constant, pf was greater with faster rotating speeds. When the rotating speed remained constant, 6-mm plastic beads had a greater pf than 6-mm glass beads (Fig. 5de), although similar pf values were observed when 4-mm particles

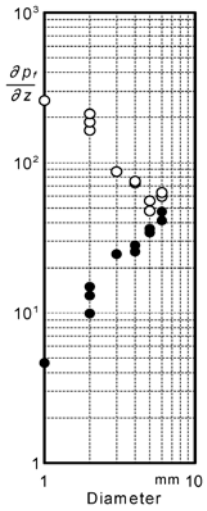

Fig. 6. - Comparison between measured (open circle) and calculated (closed circle) excess pore water pressure gradient (∂pf/∂z)

were used.

A comparison by particle size revealed that in experiments using glass beads, the greatest p_f appeared for particles sized 1 mm and 2 mm, and p_f tended to decrease with increasing particle diameter. However, the p_f for 6-mm particles was greater than that for 5-mm particles. For experiments using plastic beads, the p_f for 6-mm particles was greater than that for 4-mm particles at a rotational speed of 1.0 rps, although the difference was not large.

The p_f data for glass beads (1-6 mm) was compared using rotational speeds of 1.0 rps and 1.1 rps to investigate the effect of particle size to pf value. Although the mixture volume was identical in these experiments, flow depths of the laboratory debris flows differed according to the experimental conditions. To remove the difference in flow depth, a pf gradient was used; this was derived using the pf value at the bed (z = 0) divided by the flow depth ($\partial p_f/\partial z$) assuming a linear profile of p_f Figure 6 shows the relationship between $\partial p_f/\partial z$ and particle size; it also shows the theoretical $\partial p_f/\partial z$ obtained by substituting the experimental results (u_m, c, h) into eq. (9) at z = 0 and dividing this by flow depth h. The experimental $\partial p_f/\partial z$ decreased with increasing particle diameter when diameters ranged from 1-5 mm, while the $\partial p_f/\partial z$ increased when the diameter increased from 5 mm to 6 mm. In contrast, the theoretical $\partial p_f/\partial z$ increased with increasing particle diameter for all diameters, as expressed in eq. (9), where p_f increases in proportion to squared d, due to Reynolds stress. As a result, the experimental and theoretical values for p_f did not only differ greatly, but also showed the opposite trends in relation to diameter, with the exception of the experiments using 5- and 6-mm particles, when the p_f values were relatively similar.

DISCUSSION

PORE WATER PRESSURE IN LABORATORY DEBRIS FLOWS IN A ROTATING MILL

Before investigating pore water pressure, it was important to determine whether the properties of granular mixture flows in the rotating mill sufficiently reproduced the nature of actual debris flows. Debris flows can be roughly classified into several types using the relative flow depth (h/d) (Takahashi, 2007; Hotta & Miyamoto, 2008). According to the h/d range, the granular mixture flows we studied should be similar to boulder debris flows. However, actual debris flows never have a uniform particle size. It is noteworthy how the great diversity in particle size, especially fine sediment in pore fluid, affects the pore water pressure in actual debris flows. In addition, the flow mechanisms differ, even between a granular mixture flow maintained in a rotating mill and a steady uniform debris flow in an open channel in several ways.

In an open channel, the driving force is balanced with flow resistance at any part of the steady uniform debris flow. However, a rotating mill can only maintain a steady state, and the debris flow is necessarily non-uniform. As the granular mixture flow in the rotating mill descends on the side wall of cylinder, the bed inclination varies with location, resulting in an entirely non-uniform debris flow. Additionally, particles in the debris flow circulate within the rotating mill and counterchange between the upper and lower layers at the front and rear edges, respectively. Particles on the bed move with the rotating bed roughness and are released at the rear edge with a steep slope, 'falling' to the front part. This flow mechanism means that granular mixture flows within a rotating mill differ from actual debris flows, so the fundamental nature of the debris flow in a rotating mill might also differ from a typical debris flow evaluated by the constitutive equations.

However, the differing flow mechanisms between debris flows do not significantly affect the Reynolds stress in interstitial waterflow mechanisms. Interstitial water in debris flows is exposed to strong shearing by particles, and Reynolds stress is considered to be gov-

erned by particle motion around the interstitial water. Consequently, the Reynolds stress can be treated in the same manner for velocity profiles in a rotating mill and in an open channel.

Figure 2 shows that the velocity profiles for both glass and plastic beads were in good agreement with the typical velocity profile for a boulder debris flow over a rigid bed in an open channel. Thus, the pore water pressure in the laboratory debris flow in the rotating mill exhibits the value described in eq. (9). However, when experimental and theoretical pore water pressures are compared across the particle diameters of glass beads (Fig. 6), the measured pore water pressure did not correspond with the calculated value derived from eq. (9), especially under conditions of small-diameter beads. Thus, we investigated the source of this disagreement. Other than Reynolds stress, the following three candidates might be responsible for increasing pore water pressure in granular mixture flows within a rotating mill.

A) Increasing pore water density, due to release of internal particle-to-particle stress.

B) Centrifugal force, due to rotation.

C) Pressure gradient induced by an internal flow of interstitial water different from the track of particles.

Candidate A might result in increased pore water pressure when a debris flow descends as a turbulent flow. In a turbulent debris flow, the internal particle-to-particle stress is released as particles in the debris flow are actively mixed. A stress equivalent to the released particle-to-particle stress should be supported by interstitial water, resulting in increased apparent density. This increase in the apparent density of interstitial water can be observed as increased pore water pressure. However, in this study the velocity profile (Fig. 2) confirmed that particles in the granular mixture flow moved in a laminar fashion and no mixing of particles (even small particles) occurred, except in the front and rear edges. Figure 4 reveals slightly higher concentrations under conditions of smaller particles. This finding indicates that inter-particle contact is more dominant with smaller particles, supporting the hypothesis that debris flows with small particles should be also regarded as laminar, because particle mixing does not appear to occur under these conditions. Therefore, Candidate A can be rejected as a factor affecting the increased pore water pressure.

Candidate B is inherent in the use of a rotating mill.

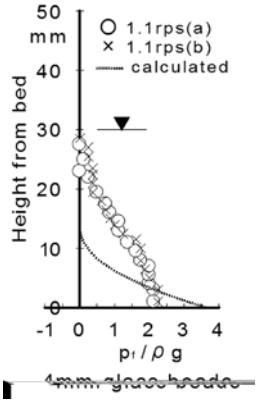

Fig.7 - Comparison between distributions of measured and centrifugally-driven excess pore water pressures

Although the velocity at the bed surface was regarded as zero for experimental purposes (Fig. 2), the bed and the flow part near the bed did actually move with the rotation of the mill. If the debris flow in the rotating mill was influenced by this rotation, centrifugal force might act as inertial force in addition to gravity, thereby increasing the pore water pressure. Considering the centrifugal force, hydrostatic pressure can be written as:

$$p_h = \rho(g + \alpha_c(z))(h - z) \quad (10)$$

$$\alpha_c(z) = u_r^2(z) / R(z) \quad (11)$$

where $u_r(z)$ is the profile of the rotational speed in the debris flow and $R(z)$ is the distance from the center axis of the rotating mill. For example, Figure 7 compares the measured distribution of excess pore water pressure with the calculated distribution by substituting the experimental conditions into eqs. (10) and (11). Although basal pore water pressure values were comparable between measured and calculated results (Fig. 7), increases in calculated pressure do not appear in the upper part (heights greater than 10 mm from the bed) of the granular mixture flow, so the profiles disagree. Also, based on eqs. (10) and (11), when centrifugal force increases the pore water pressure, the basal pore water pressure should increase to at least the same extent in experiments using the same rotating speed; this did not occur (see Fig. 5). Thus, centrifugal force does not explain the differing pore water pressures for the different particle sizes (Fig. 6).

It is important to note that the effect of the centrifugal force on pore water pressure (Fig. 7) was calculated based on the velocity profile derived from eq. (8). Although results indicated that eq. (8) fit with the actual velocity profile in the rotating mill (Fig. 2), they did not assure that the velocity of interstitial water correspond-

ed exactly to the particle velocity. Figure 3 shows that in the granular mixture flow, a clear water part was observed in front of the complex internal flow. An emerging flow was maintained from the debris flow surface, suggesting that the flow lines of particles and interstitial water did not correspond. That is, the effect of the centrifugal force might be more limited for pore water than for particles. Considering the factors discussed above, Candidate B can also be rejected as a cause of increased pore water pressure. However, as mentioned above, centrifugal force might affect particles in granular mixture flows in a rotating mill: centrifugal force is equal to roughly K to ½ the gravity near the bed of the rotating mill. Consequently, when investigating particle-to-particle stresses in debris flows in a rotating mill, the influence of centrifugal force should be taken into consideration

Candidate C should be considered when the flow lines of particles and interstitial water disagree. In the granular mixture flow in the rotating mill, an emerging flow occurred from the debris flow surface (Fig. 3) and the surfaces of the interstitial water and the debris flow also disagreed at the rear edge of the debris flow where the particles were dragged above the water surface by the bed of the rotating mill, resulting in temporary unsaturation. These results Fig. 8. Relationship between particle diameter and gradient of excess pore water pressure. Open circle indicates the measured excess pore water pressure gradient (;p_f/;z). Solid line indicates eq. (9), broken line indicates eq. (15) divided by flow depth, and dashed line indicates the sum of these. highlight the disagreement between the flow lines of particles and interstitial water in the granular mixture flow induced in the rotating mill. Because both flow lines usually correspond in a debris flow in an open channel, Candidate C is also an inherent issue related to the use of a rotating mill. Generally, the interactive force acts in such a way as to produce a difference in velocity between particles and interstitial water. When particles are sufficiently dense to be treated as porous media, this difference in velocity can be interpreted as an infiltration flow, where the interactive force is described as a pressure loss. In contrast, when the phenomenon is interpreted as the sum of single-particle motion in the fluid, the interactive force can be described as the drag force of the particles. Although the interactive force can be expressed as the pressure gradient of fluid in both situations, the latter is more applicable to this discussion of increased pore water pressure, because the former generally treats the interstitial flow as laminar.

By setting the velocity difference between the particles and interstitial water in the z direction as v in the granular mixture flow within the rotating mill, the drag force on single particle D can be expressed as

$$D = D_S + D_I \tag{12}$$

$$D_S = 3\pi\mu dv \tag{13}$$

$$D_I = \frac{9}{16}\rho\pi d^2 v^2 \tag{14}$$

where D_s is the Stokes drag, D_I is the inertial drag, and μ is the viscosity coefficient of water. D_s is dominant in flows with a small Reynolds number, while D_I exceeds D_s in flows with a large Reynolds number. Equation (12) can be rewritten as a pressure gradient using sediment concentration c as:

$$\frac{dp}{dz} = -\frac{6cD}{\pi d^3} = -\left(\frac{18c\mu v}{d^2} + \frac{27}{8}\frac{c\rho v^2}{d}\right) \tag{15}$$

From the right side of eq. (15), increased pore water pressure (derived based on Candidate C) is expressed in inverse proportion to d-squared or d. Because the excess pore water pressure is expressed in proportion to d-squared in eq. (9), a combination of eq. (9) and (15) can reproduce experimental results (Fig. 6). Substituting representational experimental conditions from Fig. 6 (rotating speed: 1.0 rps, c: 0.4) into eqs. (9) and (15), relationships between particle diameter and gradient of excess pore water pressure can be obtained (see Fig. 8). Figure 8 also shows the

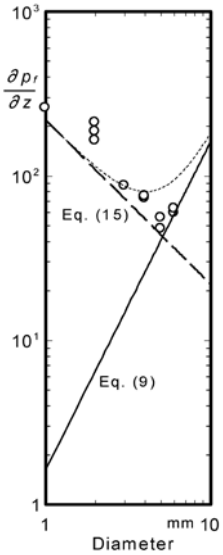

Fig.8 - Relationship between particle diameter and gradient of excess pore water pressure. Open circle indicates the measured excess pore water pressure gradient (;pf/;z). Solid line indicates eq. (9), broken line indicates eq. (15) divided by flow depth, and dashed line indicates the sum of these

results from Figure 6 and the sum of eqs. (9) and (15). The value for v in eq. (15) was obtained as 4 (cm/s) by setting eqs. (9) and (15) to cross at a 5-mm diameter, referring to the plot distribution shown in Figure 6. This value of 4 cm/s for the velocity difference between particles and interstitial water does not differ greatly from the roughly-observed velocity of the emerging flow from the surface of the granular mixture flow, supporting the theory that a combination of eqs. (9) and (15) reproduced the results shown in Figure 6 Based on Figure 8, Candidate C can explain the measured increase in pore water pressure: the pressure gradient due to the internal flow, in addition to Reynolds stress, increased the pore water pressure in the rotating mill. Some issues remain to be examined, such as whether pore pressure can be increased simultaneously based on eqs. (9) and (15) and how infiltration velocity is determined by experimental conditions. In addition, .the infiltration flow emerging from the flow front (Fig. 3) implies that a longitudinal gradient of excess pore-water pressure exists within the flow, at least in the case with small particles. It is unclear how the presence of this gradient might bias the pore-pressure measurements, which were made along a single vertical transect.

However, the most remarkable finding at this point is that the expressions for eqs. (9) and (15) are quite different as functions for d. The pressure gradient due to infiltration flow (Candidate C) and Reynolds stress can independently reproduce the increased pore water pressure for conditions of small and large particles, respectively. That is, although a factor other than Reynolds stress can increase pore water pressure in a granular mixture flow in a rotating mill, this factor's effect can be eliminated by increasing the particle diameter. In this study, pore water pressure measured using experiments with 6-mm particles increased due to Reynolds stress, based on the results shown in Figure 8. Additionally, eqs. (9) and (15) are different with regard to dependence on c. Reynolds stress increased with decreasing concentrations and excess pore water pressure due to Candidate C increasing with increasing concentration. Both factors responded oppositely to the scale of the pore space.

PORE PRESSURE AS REYNOLDS STRESS

As discussed in the previous section, the increased measured pore water pressure appeared to be induced by Reynolds stress in experiments using particles with a 6-mm diameter. Excess pore water pressure was measured and calculated using eq. (9) for all data of 6 mm particles. Figure 9 compares the measured and calculated values, which were in good agreement, although different trends appeared in the distributions between glass beads and plastic beads. Calculated values were greater than measured values for glass-bead experiments, while measured values were greater for plastic-bead experiments.

When rotational speeds were identical, the pore water pressure measured in plastic-bead experiments was greater than that in glassbead experiments (Fig. 5de). This can be explained by the lower concentrations of plastic beads than glass beads (Fig. 4), as the excess pore water pressure shown in eq. (9) increases with increasing mixing length, and the mixing length increases when concentration decreases. The experimental results revealed higher pore water pressure in the granular mixture flow of plastic beads, which had lower specific weight than glass beads. This is an important finding with regard to the internal stress structure of debris flows. It suggests that stress in the pore water of a debris flow behaves independently from particle-to-particle stresses that are related to the specific weight of the particles, and is primarily determined by the structure of the pore space. This finding might also support the assumption when modeling the constitutive equations of debris flow that internal energy dissipation occurs independently, depending on space: particle-to-particle collisions consume energy inside the beads, friction between particles consumes energy on the particle surface, and Reynolds stress due to pore fluid mixing consumes energy in the pore fluid (Egashira *et alii*, 1989).

The differing experimental and theoretical values between glass and plastic beads (Fig. 9) appear to be related to the shape of the pore space when the particle concentration changes. Assuming no increases in pore water pressure due to the infiltration flow under conditions of 6-mm particles, differences between the measured and theoretical pore water pressure can thus be considered to be caused by Reynolds stress, as shown in eq. (9). Equation (9) simply uses mixing length based on shape parameters for sediment particles and pore space, as described in eq. (4). The effective space for the mixing length can be derived from eq. (4) without considering the effect of particle concentration,

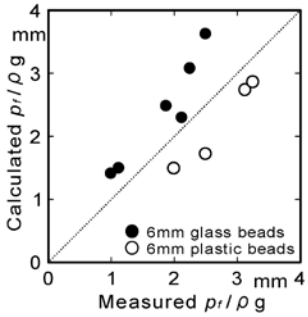

Fig. 9 - Relationship between measured and calculated basal pore water excess pressure from hydrostatic pressure

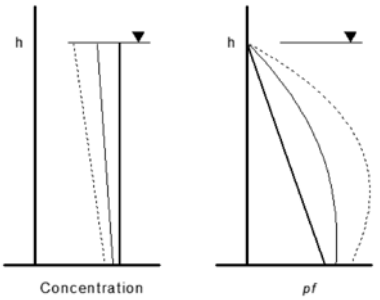

Fig.10 - Relationship between concentration profile and excess pore water pressure distribution

i.e., that is the mixing length changes in proportion to the concentration regardless of the changing shape of the pore space. However, because pore space deforms with increasing concentration, reducing the mixing length due to the decreased effective volume of the pore space, shape parameters should be expressed as functions of concentration. SUZUKI *et alii* (2003) reported that when a debris flow has a low concentration, it is preferable to use 0.08 kf rather than 0.16-0.25 k_f, as was previously proposed by ASHIDA *et alii* (1985) and EGASHIRA *et alii* (1989). EGASHIRA *et alii* (1989) also reported that a constant k_f overestimates mixing length l in case of lower sediment concentration c, and SUZUKI (2007) proposed k_f as a function of c. Together, these results suggest that mixing length is overestimated in glass beads with higher concentrations, and underestimated in plastic beads with lower concentrations, resulting in the differing results from measurement and calculation (Fig. 9).

The structure of pore space in a granular mixture flow might also affect the pore pressure profile. In this study, two types of excess pore water pressure profiles appeared: linear and parabolic (Fig. 5). The parabolic profile was obtained in cases with higher pore water pressure. Pore water pressure increased with increasing rotating speed for identically-sized particles with same specific weight. Because the mean concentration of the debris flow decreased with increasing rotating speed (Fig. 4), not only um but also c affected the increased pore water pressure, as shown in eq. (9). In eq. (9), p_f increases linearly when c is vertically uniform, while p_f profile differs from a straight line when c is non-uniform. Figure 10 shows the theoretical p_f profiles derived feom eq. (9) using three different types of c profiles. The gradient of c from surface to the bed was steeper when the mean concentration was lower. Figure 10 reproduces the shape of the pf profile, which changes from linear to parabolic when the the c profile inclines. Although this study did not measure concentration profiles, Figure 10 may explain the results in Figure 5, implying that the concentration profiles inclined with decreasing mean concentrations due to an increasing speed of rotation.

CONCLUSIONS

This study measured pore water pressure distributions in granular mixture flows in a rotating mill to investigate the internal stresses of debris flows. The experimental results revealed that the pore water pressure was greater than the hydrostatic pressure. The results imply that a Reynolds stress model best fits the data when only larger particles are present, whereas an "infiltration flow" drag model best fits the data when only smaller particles are present. A combination of the two models provides the best fit to the full dataset. The data are inconclusive as far as determining which model might work best for real debris flows with a great diversity of particle sizes.

The observed excess pore water pressure in debris flows using 6-mm particles corresponded closely to theoretical values, supporting that the theory that constitutive equations can also evaluate shear stress in pore fluid of debris flows with uniform grain size.

Differing pore water pressure profiles could be explained by the differing sediment concentration gradients, which appeared to induce uneven mixing lengths. Observed pore water pressure was greater for debris flows consisting of particles with lower specific gravity, indicating that the stress components of pore fluid behaves independently from those of sediment parti-

cle interactions, and are determined by the pore-space structure of debris flows.

ACKNOWLEDGEMENTS

I express sincere thanks to Prof. Miyamoto (University of Tsukuba) for his comments on the pore pressure measurements and the background of the constitutive equations of debris flows. This research was partially supported by the Ministry of Education, Science, Sports and Culture, Grant-in-Aid for Scientific Research, 22780140, 2010.

REFERENCES

Arai M. & Takahashi T. (1986) - *The mechanics of mud flow.* Proceedings of the Japan Society of Civil Engineers, **375** (II-6)**:** 69-77. (in Japanese with English summary)

Arattano M. & Franzi L. (2004) - *Analysis of different water-sediment flow processes in a mountain torrent,* Natural Hazards and Earth System Sciences, **4:** 783-791.

Ashida K., Egashira S., Kamiya H. & Sasaki H. (1985) - *The friction law and moving velocity of a soil block on slopes.* Annals of the Disaster Prevention Research Institute, Kyoto University, **28** (B-2)**:** 297-307. (in Japanese with English summary)

Bagnold R.A. (1954) - *Experiments on a gravity-free dispersion of large solid spheres in a Newtonian fluid under shear.* Proceedings of the Royal Society of London, Series A, Mathematical and Physical Sciences, **225:** 49-63.

Egashira S., Ashida K., Yajima H. & Takahama, J. (1989) - *Constitutive equations of debris flow.* Annals of the Disaster Prevention Research Institute, Kyoto University, **32** (B-2)**:** 487-501. (in Japanese with English summary)

Egashira S., Miyamoto K. & Itoh T. (1997) - *Constitutive equations of debris flow and their applicability.* Proceedings of the 1st International Conference on Debris-Flow Hazards Mitigation, 340-349.

Hotta N., Miyamoto K., Suzuki M. & Ohta T. (1998) - *Pore-water pressure distribution of solid-water phase flow in a rolling mill.* Journal of the Japan Society of Erosion Control Engineering, 50 (6): 11-16. (in Japanese with English summary)

Hotta N. & Ohta T. (2000) - *Pore-water pressure of debris flows.* Physics and Chemistry of the Earth (B), **25** (4)*:* 381-386.

Hotta N. & Miyamoto K. (2008) - *Phase classification of laboratory debris flows over a rigid bed based on the relative flow depth and friction coefficients.* International Journal of Erosion Control Engineering, **1** (2)**:** 54-61.

Imaizumi F., Tsuchiya S. & Ohsaka O. (2003) - *Flow behavior of debris flows in the upper stream on mountainous debris torrent.* Journal of the Japan Society of Erosion Control Engineering, **56** (2)**:** 14-22. (in Japanese with English summary)

Itoh T. & Egashira S. (1999) - *Comparative study of constitutive equations for debris flows.* Journal of Hydroscience and Hydraulic Engineering, **17** (1)**:** 59-71.

Iverson R.M. (1997) - *The physics of debris flows.* Review of Geophysics, **35** (3)**:** 245-296.

Iverson R. M., Logan M., LaHusen R.G. & Berti M. (2010) - *The perfect debris flow? Aggregated results from 28 large-scale experiments,* Journal of Geophysical Research, 115: F03005.

Krumbein W. C. (1941) - *The effects of abrasion on the size, shape and roundness of rock fragments.* Journal of Geology, **49:** 482-520.

Kuenen P.H. (1956) - *Experimental abrasion of pebbles 2. Rolling by current.* Journal of Geology, **64:** 336-368.

McArdell B.W., Bartelt P. & Kowarski J. (2007) - Field observations of basal forces and fluid pore pressure in a debris flow. Geophysical research letters, **34:** L07406.

Miyamoto K. (1985) - *Mechanics of grain flows in Newtonian fluid.* Ph.D.-thesis presented to Ritsumeikan University, Japan. (in Japanese).

O'Brien J.S. & Julien P.Y. (1988) - *Laboratory analysis of mudflow properties.* Journal of Hydraulic Engineering, **114** (8)**:** 877-887.

Rickenmann D. (1991) - *Hyperconcentrated flow and sediment transport at steep slopes.* Journal of Hydraulic Engineering, **117** (11)**:** 1419-1439.

Savage S.B. & Iverson R.M. (2003): *Surge dynamics coupled to pore-pressure evolution in debris flows.* Debris-flow Hazards Mitigation: Mechanics, Prediction and Assessment, Rickenmann D. & Chen C.L. eds., Millpress, Rotterdam, 503-514.

Shanmugam G. (1996) - *High-density turbidity currents: Are they sandy debris flows?* Journal of sedimentary Research, **66** (1)**:** 2-10.

Suzuki T., Hotta N. & Miyamoto K. (2003) - *Influence of riverbed roughness on debris flows.* Journal of the Japan Society of Erosion Control Engineering, **56** (2)**:** 5-13. (in Japanese with English summary)

Suzuki T. (2007) - *Flow mechanics of debris flows on the roughness boundary.* Ph.D.-thesis presented to the University of Tokyo, Japan. (in Japanese).

Takahashi T. (1977) - *A mechanism of occurrence of mud-debris flows and their characteristics in motion.* Annals of the Disaster Prevention Research Institute, Kyoto University**, 20** (B-2)**:** 405-435. (in Japanese with English summary)

Takahashi T. (1978) - *Mechanical characteristics of debris flow,* Journal of Hydraulic Engineering, 104, HY8: 1153-1169.

Takahashi T. (2007) - *Debris flows: Mechanics,* Prediction and Countermeasures, Taylor and Francis / Balkema, 448p.

Takahashi T. & Kobayashi K. (1993) - *Mechanics of the viscous type debris flow.* Annals of the Disaster Prevention Research Institute, Kyoto University, **36** (B-2): 433-449. (in Japanese with English summary)

Tsubaki T., Hashimoto H. & Suetsugi T. (1982) - *Grain stresses and flow properties of debris flows.* Proceedings of the Japan Society of Civil Engineers, **317:** 79-91. (in Japanese)

Winterwerp J.C., de Groot M.B., Mastbergen D.R. & Verwoert H. (1990) - *Hyperconcentrated sand–water mixture flows over flat bed,* Journal of Hydraulic Engineering, 116 (1): 36-54.